Radiation Efficiency and Sound Field Measurements on Stringed Musical Instruments

I. Perry and B. Richardson
Cardiff University, Physics and Astronomy, Queen's Buildings, The Parade, CF 24 3AA Cardiff, UK
perryia1@cardiff.ac.uk

The radiation efficiency, η, is defined as the ratio of the acoustical power output to the mechanical power input. The mechanical power input and acoustical power output were measured on a set of freely suspended stringed musical instruments in an anechoic chamber. The instruments were excited on their bridges using an instrumented impact hammer and the velocity response was measured using an accelerometer. The sound pressure response from the instrument was measured at 324 locations on two concentric measurement spheres using two microphones. The power input was determined by taking the cross power spectrum of the force and velocity. A spherical-harmonic decomposition algorithm was used to calculate the source strengths of the monopole, dipole and other higher order contributions to the radiated sound fields. Using these source strengths, the acoustical power output for each contribution was calculated. The total radiation efficiency and that of the individual components is presented in the frequency range 80 Hz to 2000 Hz. The three instruments studied were a classical guitar (BR2), a carbon fibre steel string guitar (X10) and a violin. At lower frequencies within this range the output power for all three instruments is dominated by monopole radiation. At higher frequencies the dipole components contribute more to the output power. It was found that the peak values of η do not coincide with known body modes for the two guitars. Normalised sound pressure fields are shown for frequency ranges where the sound pressure profile changes from a monopole to a dipole.

1 Introduction

Many of the previous studies on the physics of stringed instruments have focused either on input admittance measurements (velocity per unit force) across a frequency range or on the shapes and behaviours of body modes. Studies of mechanical input power and acoustical output power have previously been made on two classical guitars [1] below 550 Hz and at two separate frequencies on another classical guitar [2]. Radiated sound fields have been studied at the resonance frequencies of the body modes of a classical guitar, which had been found using holographic interferometry [3].

In this paper the radiation efficiency between 80 Hz and 2000 Hz is shown for three stringed instruments; BR2, X10 and a violin. BR2 is a handmade Torres style classical guitar, X10 is a carbon-fibre steel-string guitar and the violin was made to a standard design in a violin making school. Sound fields from BR2 are also shown away from the resonance frequencies of its body modes.

2 Radiation Efficiency

The term radiation efficiency has been used to describe several quantities within the literature. The definition used in this work is that radiation efficiency, η, is the ratio of the *acoustical* power output to the *mechanical* power input. This is the same definition used in previous studies on two classical guitars [1] and a piano sound board [4].

2.1 Mechanical power input

The mechanical power input at a frequency, ω, is measured by taking the cross power spectrum of the force, $F(\omega)$, and the velocity, $v(\omega)$, at the same point on the instrument.

$$P(\omega) = Re[F^*(\omega)v(\omega)]/2 \quad (1)$$

The factor of 2 is included in Eq. (1) because the velocity and force are RMS values. The velocity was measured by integrating the signal produced by an accelerometer and the force was both supplied and measured using an instrumented impact hammer. The impulse provided by the hammer excited the instrument across a wide range of frequencies. The upper frequency limit is determined by the hardness of both the tip of the hammer and the surface being struck. The instrument is driven at all frequencies up to that limit. Using an impact hammer allows for the instrument to be excited across a range of frequencies in a short period of time. This results in considerably quicker measurements in comparison with using frequency sweeps or filtered noise excitation. A disadvantage of using an impact hammer to provide an excitation is that it is not possible to drive the instrument at a single frequency. Individual body modes cannot be excited without driving other modes and the response at any frequency will be produced by several body modes rather than single isolated modes.

2.2 Acoustical power output

Measuring the acoustical output power is more complicated than measuring mechanical power input. One method for calculating output power is to measure the sound intensity around the instrument. Sound intensity can be measured using a single microphone but only if the radiated sound fields have a known shape. As musical instruments typically radiate non-spherical sound waves, with dipoles, quadrupoles and other higher-order components contributing to the radiated sound, this technique is not applicable. At distances much greater than the wavelength of the radiated sound, sound waves may be treated as being planar in nature. However due to restrictions imposed by the length of audio wavelengths at low frequencies and also by the size of anechoic rooms it is not often possible to make use of this simplification. Sound intensity can also be measured using a sound intensity probe which measures the sound pressure and air velocity at the same point. This allows for the study of the total power output in the near field but does not allow for measurement of the contributions of monopole, dipole and other higher-order sources to the power output.

In this paper the acoustical power output was measured using a spherical-harmonic decomposition algorithm to determine the source strengths of the different components that produce the radiated sound. The use of spherical-harmonic decomposition allows the contribution to the total power output from monopole, dipole and higher order sound sources to be determined. This technique has previously been used to calculate the source strength of the top plate modes of BR2 at their resonance frequencies [3]. The full method for spherical-harmonic decomposition can be found in reference [5] but a brief summary is provided here.

The radiated sound pressure, $p(r, \theta, \phi)$, at a single point in space at a known radius, r, and angles , θ and ϕ, from a source [6] is

$$p(r, \theta, \phi) = \sum_{lm} [a_{lm} h_l(kr) + b_{lm} h_l^*(kr)] Y_{lm}(\theta, \phi) \qquad (2)$$

where $h_l(kr)$ is a spherical Hankel function, $Y_{lm}(\theta, \phi)$ is a spherical harmonic term, k is the wave number, a_{lm} is the outgoing wave coefficient, b_{lm} is the incoming wave coefficient and l & m describe the order of the spherical harmonic. Measuring the sound pressure on two concentric spheres, with radii r_1 and r_2, allows the values of a_{lm} and b_{lm} to be calculated by solving the simultaneous equation shown in Eq. (3).

$$\begin{bmatrix} a_{lm} \\ b_{lm} \end{bmatrix} = \begin{bmatrix} h_l(kr_1) & h_l^*(kr_1) \\ h_l(kr_2) & h_l^*(kr_2) \end{bmatrix}^{-1} \begin{bmatrix} C_{lm}(r_1) \\ C_{lm}(r_2) \end{bmatrix} \qquad (3)$$

where C_{lm} is a spherical weighting calculated from the sound pressure measurements using the spherical-harmonic decomposition algorithm. The b_{lm} values are used to describe the sound waves moving towards the instrument and can be reduced by removing external sound sources and preventing reflection from the room walls. The reflections were kept to a minimum by making all of the measurements in an anechoic chamber. By calculating the outgoing coefficient, a_{lm}, the source strength, S_ω, can be determined and the acoustical power output from a monopole source, Π_s, at a single frequency, ω, can be calculated using equation Eq. (4).

$$\Pi_s = \frac{\rho \omega^2}{4\pi c} |S_\omega|^2 \qquad (4)$$

where ρ is the air density and c is the speed of sound in air. The equations for output power from dipole and higher order contributions are shown in reference [7]. The total power output is calculated by summing the power outputs produced by the monopole, dipole and other higher order components. The radiation efficiency, η, is calculated by dividing the total output power by the input power. It was found that the quadrupole contribution to the acoustical power output is negligible so it is omitted from the radiation efficiency graphs.

Eq. (2) and (3) can be used to calculate the source strength for any values of l and m providing that a suitable number of sound pressure measurements are made on the two concentric measurement spheres. If the instrument is assumed to produce only monopole sound radiation then a single measurement point is suitable to describe the sound pressure as it will be equal in all directions. For dipoles two microphone locations are required but the orientation of the dipole must also be known. In this work 36 azimuthal and 9 elevational angles were used to make pressure measurements at 324 points on two concentric spheres. Making 324 sound pressure measurements provides many more pressure values than required for determining the contributions from monopoles and dipoles. The greater number of measurements allows for a more accurate determination of the a_{lm} and b_{lm} values for $l = 0$ and $l = 1$ and also produces sound pressure fields with a high spatial resolution.

Using Eq. (3) to describe the sound pressure produces incorrect values of a_{lm} when the separation of the microphones is equal to half of the wavelength of the radiated sound. The determinant of the matrix containing the spherical Hankel functions approaches infinity as the microphone separation approaches an integer multiple of the half wavelength. This leads to exceptionally large values for the incoming and outgoing coefficients and the source strength. This only has an effect near to integer multiples of the half wavelength and at other frequencies it does not affect the calculated pressure response or output power.

3 Method

An instrumented, automated impact hammer (PCB model 086E80) was used to excite the instruments on the bridge. The velocity response was measured using an accelerometer (PCB model 352B10) and the sound pressure was recorded using two $^1/_2''$ microphones (both B&K type 4165/2619) located on two separate measurement spheres around the instrument. The hammer strike location and accelerometer were placed close to one another to produce a good approximation of input admittance and power measurements. The sound pressure generated from each hammer excitation was measured at 324 points on the surface of the measurement spheres and the corresponding force and acceleration measurements were saved as well. These measurements were all undertaken in an anechoic chamber (dimensions 2m x 2m x 1.5m). The size of the anechoic chamber limited the radii of the measurement spheres to 0.45m and 0.71m, with the instrument in the centre of the room and the measurement spheres. The instruments were suspended from a rotating central column using elastic bands around their tuning pegs. The microphones were moved through the nine elevation angles, which were calculated using Gaussian quadrature, and the instrument was rotated through the 36 points 10° at a time. The recordings from each strike were made for two seconds at a sampling rate of 44.1 kHz and a fast Fourier transform (FFT) of window size 2^{16} was made of the data. The total time taken to measure the sound pressure, force and velocity at 324 points was around 2 hours. This allowed for repeat measurements to be made on instruments under similar atmospheric conditions.

As in reference [1] any values of η which were greater than 1 are omitted from the figures. Values of $\eta > 1$ are typically produced by a sudden reduction in the measured input power rather than an increase in output power.

4 Classical guitar BR2

BR2 was excited on its bridge to the right of the top E string and the velocity response was measured between the top B and E strings. Figure 1 shows the total η, monopole η and dipole η of BR2. The monopole and dipole radiation efficiencies are defined as the ratio of the monopole and dipole output powers to the input power respectively. The labelled points in the figure signify the body modes of BR2, the nomenclature is that T is a top plate mode and B is a back plate mode. The first number indicates the number of anti-nodal regions across the instrument and the second number indicates the number of anti nodal regions parallel to the strings. If there are two modes with equal numbers of anti nodal regions then a subscript is applied to the mode number. The mode shapes and resonance frequencies for BR2 are those shown in [3].

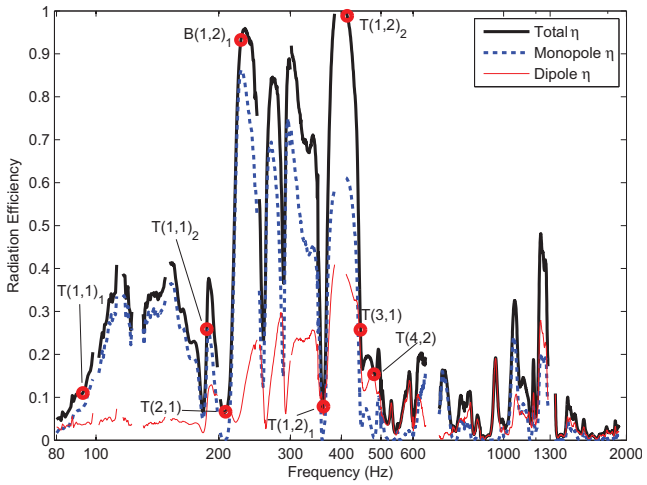

Figure 1: Radiation efficiency measured on BR2 at the top E string

There are three regions of different η behaviour for BR2 shown in figure 1. The first region is between 80 Hz and 200 Hz, the second is between 200 Hz and 450 Hz and the third is above 450 Hz. In the first region the radiation efficiency is less than 0.4 and the peak values of η do not correspond with the resonance frequencies of the modes. This region is dominated by monopole power output which is produced by the two lowest frequency body modes, $T(1,1)_1$ and $T(1,1)_2$. These modes are characterised by motion of a single anti-nodal area of the lower bout of the guitar. Both of these modes couple with the enclosed air and the back plate.

Below 200 Hz there are no body modes that radiate like dipoles but there is a dipole component produced by the $T(1,1)_1$ mode below its resonance frequency. The dipole component is produced by opposite phase motion between the sound hole and the lower bout of the top plate [8]. The dipole motion decreases with increasing frequency and therefore produces only a small amount of dipole acoustical power below 200 Hz. Body modes are known to produce a residual response above their resonance frequencies [9] but they are not excited easily at frequencies below their resonances. The dipole motion between the air and plate must therefore be the source of the dipole power output below 200 Hz rather than any of the higher frequency body modes. The final top plate mode within this region is the $T(2,1)$ mode which has two vibrating regions of equal size and opposite phase in the lower bout of the instrument. This mode has a low η value which results from a cancellation in the radiated sound pressure between the two vibrating areas and therefore a lower level of sound power output. The $T(2,1)$ mode also produces a clear dipole sound field [3]. Dipoles are less efficient radiators than monopoles and this results in the lower level of total η for this mode.

The second region shows the greatest values of η and the peak values once again do not correspond with the resonance frequencies of the body modes. Lai & Burgess [1] observed values of $\eta > 1$ between 300 Hz and 400 Hz which resulted from a low level of supplied power input. While there are values of $\eta > 1$ within this region it is a frequency range where BR2 is typically highly efficient which suggests that a sufficient power input is supplied by the impact hammer.

The peaks in η are clearly rounded unlike the sharper peaks observed at resonance frequencies in input admittance

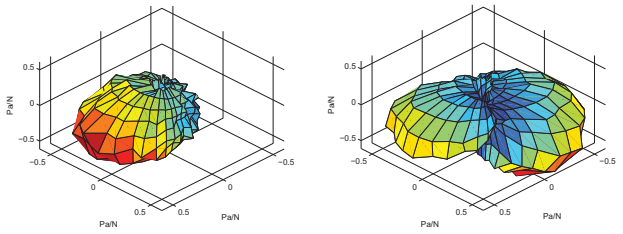

Figure 2: Radiated sound fields from BR2 at 345 Hz and 358 Hz

measurements. The rounded peaks are followed by sharp decreases in η across the entire frequency range of this second region. The decreases in η occur when there is a decrease in the monopole power output but an increase in the dipole power output. As dipoles are less efficient radiators of sound this results in an overall decrease in the total radiation efficiency. For example, the sound fields shown in Figure 2 coincide with a reduction of η from 0.67 to 0.10 between the two frequencies.

There are two $T(1,2)$ shaped modes within the second region, the first has $\eta = 0.08$ and the second has $\eta = 0.99$. These two modes have the same-shaped anti-nodal regions but they have opposite phase characteristics. The lower anti-nodal regions of the two $T(1,2)$ modes are located in the lower bout of the guitar; this is the same area where the $T(1,1)$ modes vibrate. The lower frequency $T(1,2)_1$ mode must therefore be moving with an opposite phase to the residual response of one of the $T(1,1)$ modes at its resonance frequency. The higher frequency $T(1,2)_2$ mode will be moving in phase with that $T(1,1)$ mode.

The third region of radiation efficiency has the lowest values of radiation efficiency with only 2 peaks showing $\eta > 0.25$ and other frequencies producing $\eta < 0.20$. In this frequency range there are very few modes with a monopole component and there is a greater level of sound radiation from higher-order components. The higher-frequency body modes have a greater number of smaller vibrating areas so they produce more dipole and other higher order sound radiation which results in a lower level of power output. The reduced level of radiation efficiency can also be explained by the mode shapes of the higher-frequency body modes. At frequencies above the $T(3,1)$ mode the increasing number of small vibrating areas results in one of two behaviours. If there are an even number of areas then there will be cancellation in the volume displacement which will reduce the level of power output. When there are an odd number of vibrating areas there will be some cancellation but some residual volume displacement will still occur from the remaining area. The peak in monopole sound radiation at 707 Hz is close in frequency to the $T(5,1)$ mode [10]. This mode can produce monopole sound radiation as there will be cancellation between four of the vibrating areas leaving a single small area free to vibrate and produce monopole sound radiation.

4.1 The effect of the sound hole

Blocking the sound hole of an acoustic guitar prevents a Helmholtz motion being produced in the body. The lack of a Helmholtz oscillator motion means that the $T(1,1)_1$ mode is

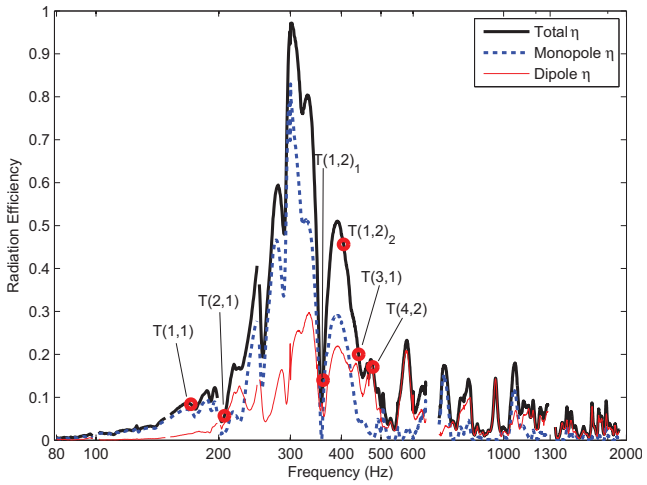

Figure 3: Radiation efficiency measured on BR2 at the top E string with the sound hole blocked

no longer present and the resonance frequency of the $T(1,1)_2$ mode is shifted downwards [11]. The effect of the sound hole on admittance and radiated sound pressure has previously been measured but its effect on radiation efficiency has not been studied.

The sound hole of BR2 was blocked using non-porous foam and the excitation and response measurements were made at the same location as when the sound hole was open. Figure 3 shows that blocking the sound hole reduces the radiation efficiency between 80 Hz and 2000 Hz. The monopole output power still dominates over the dipole output below 1000 Hz which suggests that the $T(1,1)_2$ mode is still able to produce a residual response above its resonance frequency. When the sound hole is blocked the separation between the three regions of η is not as clear but they can still be observed in the same frequency ranges as when the sound hole is open.

The first region, between 80 Hz and 200 Hz, now has values of $\eta < 0.15$. The $T(1,1)_1$ mode is no longer able to vibrate and the lowest frequency body mode is the $T(1,1)_2$ mode at 171 Hz. Below this frequency the radiation efficiency is near to 0 as there are no body modes producing a response below the $T(1,1)_2$ mode. The $T(2,1)$ mode shows the same value of η when the sound hole is blocked which suggests that this mode is not affected by the residual response from either of the two $T(1,1)$ modes.

The second region of η behaviour shows that the radiation efficiency has been reduced, with much lower peak values present. The radiation efficiency is still dominated by monopole sound radiation which is produced by the $T(1,1)_2$ mode above its resonance frequency. The two $T(1,2)$ modes have the same η characteristics with the lower frequency mode having a lower radiation efficiency ($\eta = 0.14$) than the higher frequency mode ($\eta = 0.46$). As the $T(1,1)_1$ mode cannot vibrate and the higher frequency $T(1,2)$ mode has a much lower value of η the residual response from the $T(1,1)_1$ mode must therefore have an effect on the $T(1,2)_2$ mode.

In the third region the average value of η is lower than when the sound hole is open. The most likely cause of this reduction in radiation efficiency is that the $T(1,1)_1$ mode is no longer able to provide a residual response at higher frequencies and therefore cannot strengthen the power output.

5 Steel-string guitar X10

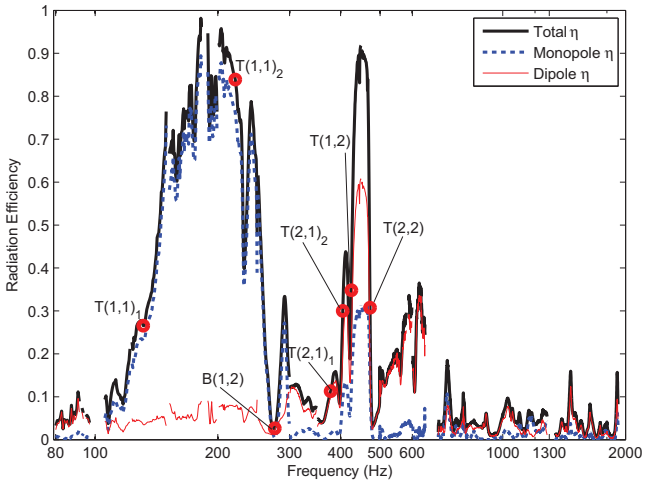

Figure 4: Radiation efficiency measured on X10 at the top E string

X10 was excited on its bridge to the right of the top E string and the velocity response was measured between the top B and E strings. X10 has curved carbon-fibre top and back plates, a cutaway body shape and an asymmetric bridge design. A steel truss rod is located within the neck to provide additional stiffness to the neck. The body mode shapes and resonance frequencies were found using a 3D scanning laser vibrometer.

X10 does not show the same three regions of η behaviour that were seen for BR2 and the greatest values of radiation efficiency occur between the two $T(1,1)$ modes. Below 300 Hz the power output is dominated by monopole radiation as there are no dipole like body modes within this region. The $T(2,1)$ mode shows a low efficiency value for X10 in the same way as BR2 due to the similarity of the mode shape on both instruments. However, at higher frequencies dipole sources provide a greater contribution to the radiated sound than the monopole sources. It would therefore appear that the $T(1,1)$ modes do not produce a residual effect across as wide a frequency range for X10 as for BR2. This can be explained by the fact that steel-string guitars have a stiffer construction than nylon-string guitars to support the higher tension steel strings. Any mode will produce a lower amplitude residual response above its resonance frequency because of the higher stiffness of the top plates in comparison to nylon-string guitars. The values of η above 600 Hz are similar to those for BR2 so the steel string guitar is also much less efficient at higher frequencies than at lower frequencies.

6 Violin

The violin was excited on the treble side of the bridge and the impulse was provided in the same direction as the force would applied by bowing. The velocity response was measured just below the excitation point.

In figure 5 the radiation efficiency of the violin below 200 Hz is close to 0; this is an expected result as the

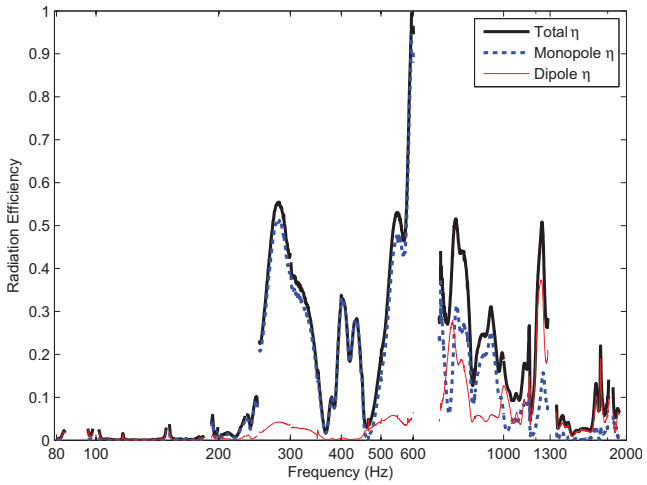

Figure 5: Radiation efficiency measured on the violin at the treble side of the bridge

lowest-frequency body mode of this particular violin is at 218 Hz. The lowest note on a violin is G_3 which has a fundamental frequency of 196 Hz, so the fundamental will not radiate sound efficiently. The resonance frequencies of the body modes of the violin do not correspond with a particular η characteristic, as seen for BR2 and X10. The monopole contribution to the power output between 200 Hz and 700 Hz is much greater than that produced by dipole components. However between 1000 Hz and 2000 Hz the radiation efficiency is dominated by dipole contributions. Above 1000 Hz the mode shapes are more complex and therefore produce dipole and higher-order radiated sound fields. The mode shapes for this particular instrument are not known but the body modes measured on another violin [12] show that several of the more complex body modes on violins below 1000 Hz have nodal lines located at the feet of the bridge. Any excitation made on the bridge will therefore excite the instrument less than if the feet were located at an anti-nodal region. These modes would be expected to be present between 200 Hz and 700 Hz. The strong monopole component and minimal dipole contribution within this range suggests that the modes cannot be easily set into motion and therefore the monopole contribution still dominates the output power.

7 Conclusions

The low-frequency η is dominated by monopole power output for all three instruments and the values of η are close to 0 below the resonance frequency of the lowest-frequency body mode. The highest values of η occur when the strongest contribution to the radiated sound is produced by monopole sound radiation. The resonance frequencies of body modes do not correspond with a particular η characteristic, instead it is the shape and phase relationship of the mode that affects its η value. Higher-frequency body modes produce more dipole sound radiation than monopole radiation due to the increased number of smaller vibrating areas.

For both guitars the $T(2,1)$ mode has a low radiation efficiency; this is a result of a cancellation in the sound pressure output between the two vibrating areas on the lower bout of the instrument. The radiated sound fields alone cannot be used to determine the level of power output from the instrument. The monopole and dipole sound fields measured from BR2 at 345 Hz and 358 Hz both have similar peak values of sound pressure but the monopole produces $\eta = 0.67$ while the dipole gives $\eta = 0.10$.

Acknowledgements

We acknowledge financial support from the EPSRC for Ian Perry. Thanks to Jimmy O'Donnell for the loan of the X10 steel-string guitar.

References

[1] J. Lai, M. Burgess, "Radiation efficiency of acoustic guitars", *Journal of the Acoustical Society of America* **88**(3), 1222–1227 (1990)

[2] J. A. Torres, R. R. Boullosa, "Radiation efficiency of a guitar top plate linked with edge or corner modes and intercell cancellation", *Journal of the Acoustical Society of America* **130**(1), 546 – 556 (2011)

[3] T. J. W. Hill, B. E. Richardson, S. J. Richardson, "Acoustical parameters for the characterisation of the classical guitar", *Acta Acustica with Acustica* **90**, 335 – 348 (2004)

[4] H. Suzuki, "Vibration and sound radiation of a piano soundboard", *Journal of the Acoustical Society of America* **80**(6), 1573 – 1582 (1986)

[5] S. J. Richardson, *Acoustical Parameters for the Classical Guitar*, Ph.D. thesis, Cardiff School of Physics and Astronomy (2001)

[6] G. Weinreich, E. B. Arnold, "Method for measuring acoustic radiation fields", *Journal of the Acoustical Society of America* **68**(2), 404 – 411 (1980)

[7] P. M. Morse, K. U. Ingard, *Theoretical Acoustics*, McGraw-Hill (1968)

[8] G. Weinreich, "Sound hole sum rule and the dipole moment of the violin", *Journal of the Acoustical Society of America* **77**(2), 710 – 718 (1985)

[9] B. E. Richardson, H. Johnson, A. D. Joslin, I. A. Perry, "The three-mass model for the classical guitar revisited", in "Proceedings of the Acoustics 2012 Nantes Conference", 2771 – 2776 (2012)

[10] B. E. Richardson, *A Physical Investigation into some factors affecting the musical performance of the guitar*, Ph.D. thesis, University College, Cardiff (1982)

[11] O. Christensen, B. B. Vistisen, "Simple model for low-frequency guitar function", *Journal of the Acoustical Society of America* **68**(3), 758 – 766 (1980)

[12] J. Moral, E. Jansson, "Eigenmodes, input admittance and the function of the violin", *Acustica* **50**(5), 329 – 337 (1982)